Non-equilibrium transport in a series of quantum dots

2006 J. Phys.: Condens. Matter 18 10269

(http://iopscience.iop.org/0953-8984/18/45/013)

INSTITUTE OF PHYSICS PUBLISHING JOURNAL OF PHYSICS: CONDENSED MATTER

J. Phys.: Condens. Matter **18** (2006) 10269–10278 doi:10.1088/0953-8984/18/45/013

Non-equilibrium transport in a series of quantum dots

Qing-Qiang Xu and Shi-Jie Xiong

National Laboratory of Solid State Microstructures and Department of Physics, Nanjing University, Nanjing 210093, People's Republic of China

Received 6 June 2006, in final form 26 September 2006
Published 27 October 2006
Online at stacks.iop.org/JPhysCM/18/10269

Abstract

We investigate non-equilibrium transport properties in a series of quantum dots in which the Kondo resonance is influenced by the coupling between dots. Based on the Anderson Hamiltonian in the strongly interacting limit, we show the splitting of the Kondo resonance at the Fermi surface and the appearance of negative differential conductance when the magnitude of the interdot coupling is in the order of the coupling between the dots and the leads. We illustrate the relationship between the negative differential conductance and the local densities of states at the dots under different biases. We also show the profile of energies of dots in the series when a finite bias is applied. Furthermore, the differences in transport properties between even and odd numbers of quantum dots in the series are investigated.

(Some figures in this article are in colour only in the electronic version)

1. Introduction

Because of a strong antiferromagnetic interaction between conduction band electrons in electrodes and localized spin in quantum dots (QDs) via high-order hopping processes, the Kondo effect, characterized by resonant tunnelling at the Fermi surface, is often observed in systems with a QD embedded between two electrodes. As a consequence, the conductance is enhanced below the characteristic temperature, the Kondo temperature T_K [1, 2]. Recently, the Kondo effect in novel systems, such as quantum dots, quantum wires, and carbon nanotubes, has been extensively studied both theoretically and experimentally. The phenomena predicted by early theories [3, 4] have been successfully observed in experiments [1, 2]. The related phenomena, such as the Coulomb blockade transport, and the interplay between the Kondo effect with other physical factors, such as the Aharanov–Bohm effect, the Fano effect, and the Josephson effect, have also been investigated [5–10]. The phenomena related to such interplay are expected to be observed in more complicated systems and at lower temperatures. Recent progress in experimental technique seems to make it possible to realize the required conditions.

The transport properties of coupled quantum dots have also attracted much attention. Aono and co-workers [11–13] and Georges and Meir [14] employed an infinite-U slave-boson mean-field theory to investigate the interplay between the Kondo effect and the antiferromagnetic

correlation. Aguado and Langreth [15] generalized this method to an out-of-equilibrium situation. Izumida and Sakai investigated the tunnelling conductance through two QDs by using the numerical renormalization group (NRG) method [16]. Büsser *et al* calculated the conductance and spin–spin correlation of two QDs by numerical diagonalization [17]. It is revealed that in a coupled double-dot system the conductance is characterized by the competition between the dot–dot tunnelling coupling and the level broadening in the dots governed by the dot–lead coupling. The Kondo resonance peak may be split when the dot–dot coupling, which leads to the formation of 'molecular' levels, is larger than the level broadening. Sánchez and Lópezthe investigated the non-equilibrium transport properties of a three-terminal QD [18]. The transport properties near equilibrium in series of three or four quantum dots at low temperatures have recently been theoretically studied [19]. Experimentally, the split of the Kondo peak in the $\mathrm{d}I/\mathrm{d}V$–V curves was observed in recent measurements [20–22].

To explore the effect of interplay between the Kondo resonance and the interdot hopping, knowledge of the non-equilibrium properties, such as the dependence of the differential conductance on the bias voltage, and the spectral density away from the Fermi level, is necessary. One may ask certain questions, namely, to what extent is the many-body Kondo state robust against the interdot tunnelling processes in systems with many QDs, and how does the number of quantum dots influence the non-equilibrium transport properties? To answer these questions, in this paper we consider several series of QDs with a single energy level ε_0 and interdot coupling t attached to two leads. Interdot coupling lifts the energy degeneracy, yielding a spreading of energy levels in the range $\varepsilon_0 \pm t$. When t is greater than the width of the Kondo resonance Γ, the resonance peak of the spectral density at the Fermi surface is expected to be broadened and to exhibit a splitting. Similarly, in the case of strong interaction one can also expect the conductance to be affected by the combined effect of the leads and the interdot coupling when the coupling t is the order of the dot–lead hopping. Compared with the results of the double-dot system, near equilibrium the effect of changing the dot–dot coupling on the Kondo resonance is different for odd and even dot numbers, while in non-equilibrium more structures appear in the curves of differential conductance versus the bias voltage if the number of dots is larger than 2 and the dot–dot coupling is stronger than the level broadening.

2. Model

The purpose of the present work is to investigate the non-equilibrium transport through a series of M quantum dots in the limit of strong on-site Coulomb interaction $U \to \infty$ coupled via hopping $V_{k\alpha}$ to two reservoirs labelled by $\alpha = \{L, R\}$ with chemical potentials μ_L and μ_R. We adopt the infinite-U slave-boson mean-field (SBMF) method [15, 23] by introducing the slave-boson operator $b_j^\dagger$ (b_j) that creates (annihilates) an empty state and the pseudofermion operator $f_{j\sigma}^\dagger$ ($f_{j\sigma}$) that creates (annihilates) a singly occupied states with spin σ in dot j. The annihilation operator of an electron in dot j is $c_{j\sigma} = b_j^\dagger f_{j\sigma}$. To eliminate the possibility of double occupancy we impose the constraint $\sum_\sigma f_{j\sigma}^\dagger f_{j\sigma} + b_j^\dagger b_j = 1$. Hence, the Hamiltonian of M quantum dots connected to leads is written as

$$\begin{aligned} H = &\sum_{k\alpha\sigma} \varepsilon_{k\alpha\sigma} c_{k\alpha\sigma}^\dagger c_{k\alpha\sigma} + \sum_{i=1}^{M} \sum_{\sigma} \varepsilon_0 f_{i\sigma}^\dagger f_{i\sigma} + \frac{1}{\sqrt{N}} \sum_{k\sigma} (V_{kL} c_{kL\sigma}^\dagger b_1^\dagger f_{1\sigma} \\ &+ V_{kR} c_{kR\sigma}^\dagger b_M^\dagger f_{M\sigma} + \mathrm{H.c.}) + \frac{1}{N} \sum_{j=1}^{M-1} \sum_{\sigma} (t f_{j+1\sigma}^\dagger b_{j+1} b_j^\dagger f_{j\sigma} + \mathrm{H.c.}) \\ &+ \sum_{j=1}^{M} \lambda_j (b_j^\dagger b_j + \sum_{\sigma} f_{j\sigma}^\dagger f_{j\sigma} - 1), \end{aligned} \tag{1}$$

where $c^{\dagger}_{k\alpha\sigma}$ ($c_{k\alpha\sigma}$) is the creation (annihilation) operator for an electron in state k with spin $\sigma = \{\uparrow, \downarrow\}$ in lead α. The last term is from the single-occupation constraints in QDs js with associated Lagrange multipliers λ_js. ε_0 is the energy level in QDs and t is the interdot coupling. For a realistic system the Coulomb repulsion U is finite, but if U is much larger than the dot–lead coupling, the deviation from the result of infinite U is only a small quantity proportional to the square of the ratio of the dot–lead coupling strength to U.

The solution of Hamiltonian (1) can be found by the use of the SBMF approach, which is an approximation to the leading terms in the $1/N$ expansion, with an extension to deal with the non-equilibrium situations [15, 23]. The bosonic operators b_js are replaced by their expectation values, $\tilde{b}_j = \langle b_j(t)\rangle/N$. Here $N = 2$ is the fold of the Hamiltonian. By calculating the equation of motion and taking into account the constraints, we arrive at

$$\sum_{k\sigma} \tilde{V}_{k,L,\sigma} G^{<}_{L\sigma,1\sigma}(t,t) + t\left|\tilde{b}_1\right|\left|\tilde{b}_2\right| G^{<}_{2\sigma,1\sigma}(t,t) = -\mathrm{i}N\lambda_1\left|\tilde{b}_1\right|^2, \tag{2}$$

$$\sum_{k\sigma} \tilde{V}_{k,R,\sigma} G^{<}_{R\sigma,M\sigma}(t,t) + t\left|\tilde{b}_{M-1}\right|\left|\tilde{b}_M\right| G^{<}_{M-1\sigma,M\sigma}(t,t) = -\mathrm{i}N\lambda_M\left|\tilde{b}_M\right|^2, \tag{3}$$

$$t\left|\tilde{b}_{j-1}\right|\left|\tilde{b}_j\right| G^{<}_{j-1\sigma,j\sigma}(t,t) + t\left|\tilde{b}_{j+1}\right|\left|\tilde{b}_j\right| G^{<}_{j+1\sigma,j\sigma}(t,t) = -\mathrm{i}N\lambda_j\left|\tilde{b}_j\right|^2 \quad \text{for } j \neq 1, M, \tag{4}$$

$$\sum_{\sigma} G^{<}_{j\sigma,j\sigma}(t,t) = \mathrm{i}\left(1 - N\left|\tilde{b}_j\right|^2\right). \tag{5}$$

Here, we define the symbol $\tilde{V}_{k,L(R),\sigma} = |b_{1(N)}|V_{k,L(R),\sigma}$, the Green function $G^{<}_{L\sigma,1\sigma}(t,t) = \mathrm{i}\langle c^{\dagger}_{kL\sigma}(t) f_{1\sigma}(t)\rangle$ and $G^{<}_{p\sigma,q\sigma}(t,t) = \mathrm{i}\langle f^{\dagger}_{p\sigma}(t) f_{q\sigma}(t)\rangle$, with p and q being labels of QDs. $G^{<}_{p\sigma,q\sigma}(\varepsilon)$ is the Fourier transform of $G^{<}_{p\sigma,q\sigma}(t,t)$, which can be viewed as elements of an $M \times M$ matrix $G^{<}_{\sigma}(\varepsilon)$.

The Green function $G^{<}_{\sigma}(\varepsilon)$ can be calculated from the Keldysh equation [24]:

$$G^{<}_{\sigma}(\varepsilon) = G^{\mathrm{R}}_{\sigma}(\varepsilon)\Sigma^{<}_{\sigma}G^{\mathrm{A}}_{\sigma}, \tag{6}$$

where $G^{\mathrm{R(A)}}_{\sigma}(\varepsilon)$ is the retarded (advanced) Green function in the quantum dot regime represented in the form of an $M \times M$ matrix. $G^{\mathrm{R(A)}}_{\sigma}(\varepsilon)$ can be calculated with the help of the equation of motion of the operators [24, 25]. $\Sigma^{<}_{\sigma}$ is the $M \times M$ self-energy matrix, and its matrix elements are

$$\Sigma^{<}_{p\sigma,q\sigma} = \mathrm{i}\tilde{\Gamma}^{\sigma}_{L} f_L(\varepsilon), \qquad \text{for } p = q = 1, \tag{7}$$

$$\Sigma^{<}_{p\sigma,q\sigma} = \mathrm{i}\tilde{\Gamma}^{\sigma}_{R} f_R(\varepsilon), \qquad \text{for } p = q = M, \tag{8}$$

$$\Sigma^{<}_{p\sigma,q\sigma} = 0, \qquad \text{otherwise}, \tag{9}$$

where $\tilde{\Gamma}^{\sigma}_{L(R)} = |\tilde{b}_{1(M)}|^2\Gamma^{\sigma}_{L(R)}$ is the renormalized coupling between the $L(R)$ lead and the QDs with $\Gamma^{\sigma}_{L(R)} = 2\pi\mathrm{i}\sum_k |V_{kL(R)\sigma}|^2\delta(\varepsilon - \varepsilon_{kL(R)\sigma})$, and $f_{L(R)}(\varepsilon)$ is the Fermi statistical function in lead $L(R)$. In what follows, $\Gamma^{\sigma}_{L(R)}$ is taken as a constant for $-D \leqslant \varepsilon \leqslant D$. It has been assumed that the lower and upper edges of the electron band at zero bias are $-D$ and D, respectively. $G^{<}_{L(R)\sigma,1\sigma}(\varepsilon)$, the Fourier transform of $G^{<}_{L(R)\sigma,1\sigma}(t,t)$, can be cast in terms of $G^{<}_{\sigma}(\varepsilon)$:

$$G^{<}_{L\sigma,1\sigma}(\varepsilon) = \tilde{V}_{k,L,\sigma}[G^{\mathrm{R}}_{1\sigma,1\sigma}(\varepsilon)g^{<}_{kL,\sigma}(\varepsilon) + G^{<}_{1\sigma,1\sigma}g^{\mathrm{A}}_{kL,\sigma}(\varepsilon)], \tag{10}$$

$$G^{<}_{R\sigma,1\sigma}(\varepsilon) = \tilde{V}_{k,R,\sigma}[G^{\mathrm{R}}_{M\sigma,M\sigma}(\varepsilon)g^{<}_{kR,\sigma}(\varepsilon) + G^{<}_{M\sigma,M\sigma}g^{\mathrm{A}}_{kR,\sigma}(\varepsilon)], \tag{11}$$

where the Green function $g^{<,A}_{kL(R)\alpha,\sigma}(\varepsilon)$ for the leads is defined as

$$g^{<}_{kL(R),\sigma}(\varepsilon) = 2\pi\mathrm{i}\delta(\varepsilon - \varepsilon_{kL(R),\sigma})f_{L(R)}(\varepsilon), \tag{12}$$

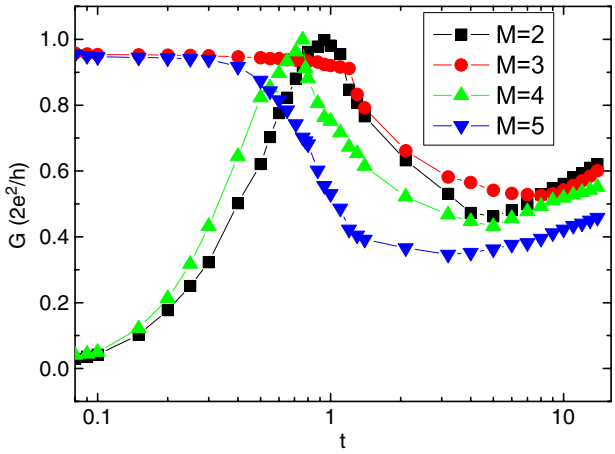

Figure 1. Interdot-hopping dependence of the linear conductance in cases with different numbers of quantum dots.

$$\sum_k g^{\mathrm{A}}_{kL(R),\sigma}(\varepsilon) = \frac{\mathrm{i}}{2}\Gamma^{\sigma}_{L(R)}. \tag{13}$$

Equations (2)–(5) form a closed set of $2M$ equations for $2M$ unknowns ($\tilde{b}_1, \tilde{b}_2, \ldots, \tilde{b}_M$ and $\lambda_1, \lambda_2, \ldots, -\lambda_M$). These equations are nonlinear and need a self-consistent solving. In this paper we perform the numerical calculation by the use of the gradient algorithm. From the solution of equations (2)–(5), we can calculate the current crossing the dots:

$$I = (-e/\pi\hbar)\,\mathrm{Im}\sum_{\sigma}\Gamma^{\sigma}_{L}\int[2G^{r}_{1\sigma,1\sigma}(\varepsilon)f_L(\varepsilon) + G^{<}_{1\sigma,1\sigma}(\varepsilon)]\,\mathrm{d}\varepsilon. \tag{14}$$

In the next section we will mainly present the non-equilibrium results for $\mu_L = -\mu_R = eV/2$, with parameters $\Gamma^{\uparrow}_L = \Gamma^{\downarrow}_L = \Gamma^{\uparrow}_R = \Gamma^{\downarrow}_R = \Gamma/2$, and $\varepsilon_0 = -2\Gamma$. The Kondo temperature of the QD is about $10^{-1}\Gamma$. The energy zero is set at the Fermi surface $E_{\mathrm{F}} = 0$. Hereafter we will use Γ as the energy unit.

3. Results and discussion

In a double-dot system the competition between the interdot hopping and dot–lead coupling plays an important role in the transport near equilibrium [12]. In order to illustrate the interplay between the Kondo effect and the interdot hopping in the case of multiple dots, in figure 1 we show the interdot-hopping dependence of the linear conductance at a given renormalized dot–lead coupling ($\Gamma = 1$) in cases of different numbers of QDs. One can see two scenarios when the interdot hopping increases. For $M = 3$ and 5, G reaches a maximum at around $t \simeq 0$. When t increases, G decreases slowly and then grows after a minimum. For $M = 2$ and 4, G increases from zero and reaches a maximum at around $t = 1$ and then decreases. When t increases further the curve becomes increasing again. In the case of $M = 2$, the previous results show that G decreases with t for large t in the case of finite U [16, 17, 26], but this dependence is reversed at the limit $U \to \infty$. This is consistent with the present results for all investigated M at the limit $U \to \infty$. The similarity for $M = 2$ and $M = 4$ or for $M = 3$ and $M = 5$ in the whole range of t can be explained from the following simple picture: at the linear limit the conductance can be written as $G = \frac{2e^2}{h}4|G_{1,M}|^2$. In the case of odd dots ($M = 3$

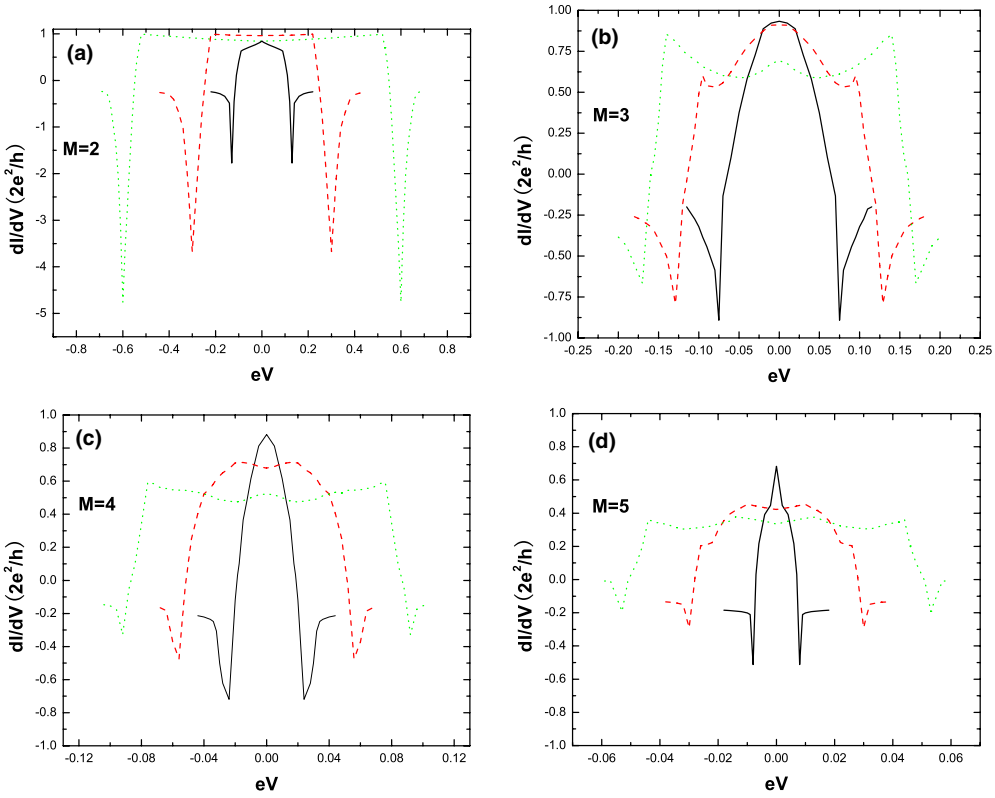

Figure 2. Differential conductance G versus bias voltage eV for different values of interdot hopping t and different numbers M of QDs. $t = 0.8, 1.2$ and 1.5 for solid, dashed, and dotted lines, respectively.

and $M = 5$) and in the Kondo regime, if the interdot hopping is not too large, the spin of the isolated series is $1/2$ and the ground state of the coupled dot–lead system is the Kondo singlet. The conductance can be calculated as $G = \frac{2e^2}{h}\frac{4\tilde{\Gamma}_L\tilde{\Gamma}_R}{(\tilde{\Gamma}_L+\tilde{\Gamma}_R)^2} = \frac{2e^2}{h}$ because $\tilde{\varepsilon}_1 \simeq 0, \ldots, \tilde{\varepsilon}_M \simeq 0$ and $|G^r_{1,M}| = \frac{1}{\tilde{\Gamma}_L+\tilde{\Gamma}_R}$. By increasing t, the levels are split and the Kondo resonance is weakened. In the case of even dots ($M = 2$ and $M = 4$), the net spin of the isolated series is about zero, leading to the vanishing Kondo resonance for small t, and the t-dependence of the conductance can be approximately calculated as $G = \frac{2e^2}{h}\frac{4\tilde{\Gamma}_L\tilde{\Gamma}_R t^2}{(t^2 b_1^2+\tilde{\Gamma}_L)^2} = \frac{2e^2}{h}\frac{4t^2}{(1+t^2)^2}$ from $|G^r_{1,M}| = \frac{t}{t^2 b_1^2+\tilde{\Gamma}_L}$. In all cases the curves are not monotonic and they show some types of oscillation. In fact, the evolution of the linear conductance in varying t shown in figure 1 is similar to the conductance oscillations with different periods in transition-metal atomic chains revealed in [27] by using combined *ab initio* and self-consistent parameterized tight-binding calculations.

In figures 2(a)–(d), we show the differential conductance G for different numbers of quantum dots ($M = 2, 3, 4, 5$) and different interdot hopping strengths $t = 0.8, 1.2, 1.5$, as a function of the bias voltage eV. From the dependence of G on the bias voltage one can see how the Kondo effect is affected by the change of the interdot tunnelling t. In the case of relatively small hopping ($t = 0.8$), the zero-bias peak of G does not split and it has a maximum intensity $G \simeq 1$, representing typical Kondo resonance at the Fermi surface. On increasing the absolute value of eV, G decreases and exhibits sharp dips associated with the negative

differential conductance (NDC). The NDC is due to the non-coincidence of resonances of the QDs in the series by increasing the bias. For $t = 1.2$, G at zero bias becomes slightly smaller than the maximum value and the Kondo resonance peak begins to split. The value of eV at which the NDC occurs is larger than the value in the case of $t = 0.8$, implying the increase of the spacing of 'molecular' levels by increasing t. For $t = 1.5$, the peak of G between two dips becomes even wider, and several small structures appear in the peak. As can be seen from the comparison of figures 2(a)–(d), the increase of the number of QDs in the series leads to stronger suppression of the resonance peak at zero bias by increasing t, which can be ascribed to a weaker Kondo effect when more quantum dots are included and play the role of one Kondo impurity. As a result of this weakening of the Kondo effect, the total width of the peak is also decreased by increasing the number of dots, M. It should be noted that for the same interdot hopping t the position where the NDC occurs strongly depends on the number of quantum dots. When the number of QDs increases and the interdot hopping is unchanged, the non-coincidence of resonances of QDs in the series happens in smaller bias, resulting in the smaller value of eV at which the NDC occurs. The small structures of the peak in the case of larger t can be attributed to the level structures of the multidot system. On increasing M, the number of levels increases, leading to an increase of small peaks in the structures.

The structures of the zero-bias peak of the differential conductance can be further understood as follows. Near equilibrium the renormalized energies $\tilde{\varepsilon}_i \equiv \varepsilon_i + \lambda_i$ on the dots are nearly zero for all i due to the screening of the conduction electrons. From this we can derive that the Kondo level is split into three molecular states, $E_1 \simeq 0$ and $E_{2,3} \simeq \pm\sqrt{2}t\tilde{b}_1\tilde{b}_2$, in the case of $M = 3$ and is split into four molecular states, $E_{i=1,2,3,4} \simeq \frac{\pm t\tilde{b}_2^2 \pm \sqrt{t^2\tilde{b}_2^4 + 4t^2\tilde{b}_1^2\tilde{b}_2^2}}{2}$, in the case of $M = 4$. In both cases the splitting of the Kondo level is of the order of $\Delta \sim 2t\tilde{b}_{1(2)}^2$. A similar result can be obtained in the case of larger M. At the same time, the width of the zero-bias peak of the differential conductance is determined by the dot–lead coupling and is of the order of $10^{-1}\Gamma$. So we can estimate a criterion $\Delta \gtrsim 10^{-1}\Gamma$ for the observation of the splitting of the zero-bias peak. When the interdot hopping t is small enough, the energy splitting is smaller than $10^{-1}\Gamma$; no splitting could be seen. When t is large, the peak of the differential conductance at $V = 0$ may be suppressed. This is just the behaviour shown in figure 1.

In order to illustrate the details of spatial and energy distributions of states in the series of QDs, in figure 3 we plot the local densities of states on the dots in the case of $M = 3$ with different bias voltages and interdot hoppings. Generally there are three main peaks, denoted by I, II, and III in figure 3(a), corresponding to the ground, the first and the second excited states, respectively. By keeping the bias voltage and comparing the densities of states with different t, we can see that the spacings of these peaks increase by increasing the interdot hopping. This behaviour can be viewed as the origin of the peak splitting in the conductance. The weights on different dots of a given state are different due to the applied bias. Usually a state with higher energy has larger weight on the dot attached to the lead with higher bias potential, but the total weight of all states on the middle dot is dominant over those on the side dots. By increasing the bias the distribution of weights for a given state among the dots becomes more inhomogeneous. The dc conductance under a bias eV depends on the total density of states within energy window $[-eV/2, eV/2]$. If it is decreased by increasing the bias, a negative differential conductance appears. It can be seen from figure 3 that the NDC may occur at relatively large bias voltage since for large eV the total density of states in the middle energy range is decreased by increasing eV due to the redistribution of the state weights on the dots.

At a finite bias we calculate the differential conductance by setting a symmetric voltage drop of two leads, i.e., $\mu_L = -\mu_R = eV/2$. The energies on the quantum dots in the series are determined self-consistently. In order to illustrate the potential profile in the dot series in

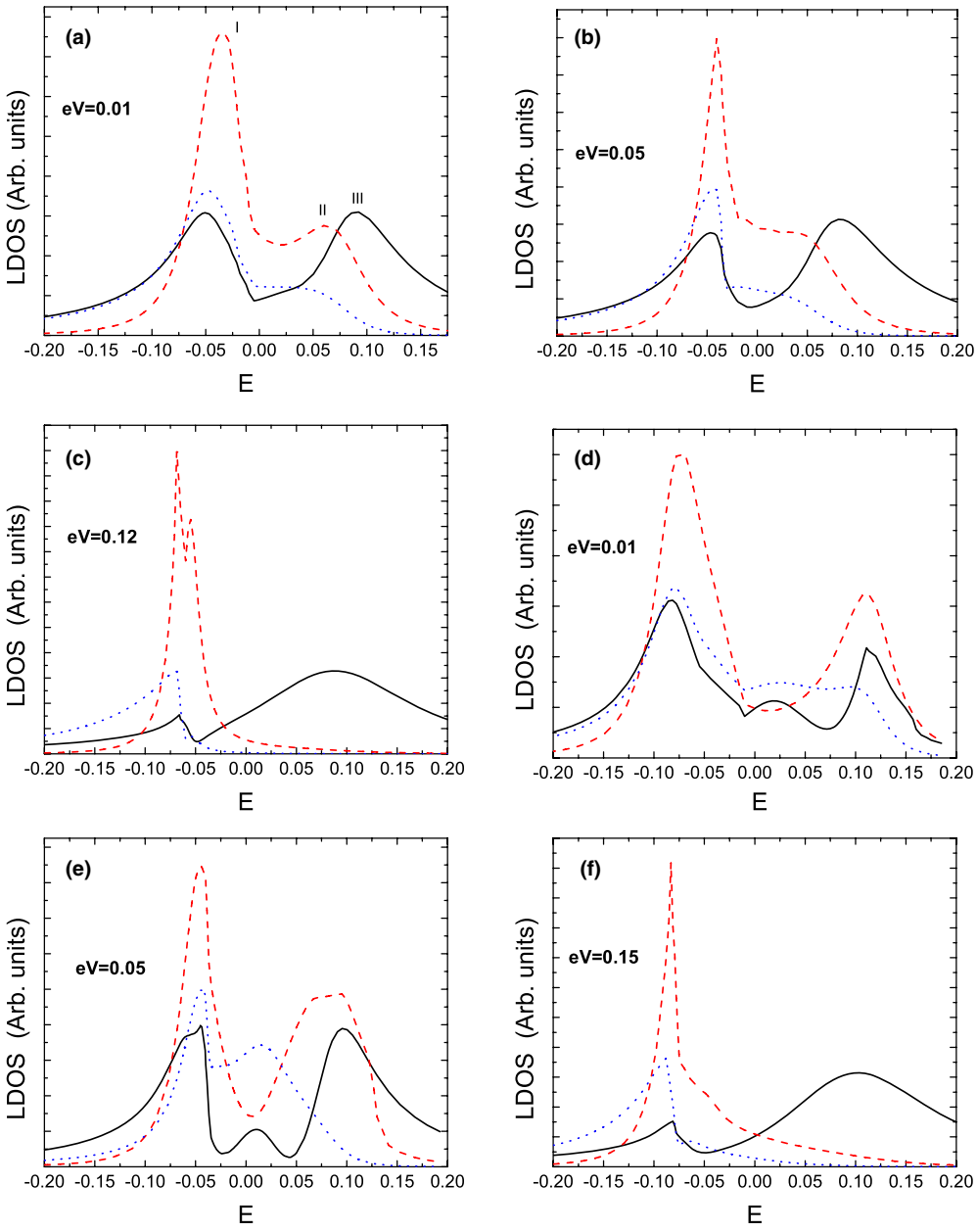

Figure 3. Local density of states in a system with three QDs for $t = 0.8$ ((a)–(c)) and $t = 1.2$ ((d)–(f)) as a function of electron energy E. Solid, dashed, and dotted lines correspond to local density of state on the left, middle, and right dots, respectively.

the non-equilibrium case, in figures 4(a) and (b) we show the renormalized energies on the dots versus the bias applied to two leads in the case of four dots with interdot hopping $t = 0.8$ and 1.2, respectively. The renormalized energy at site i is defined as $\tilde{\varepsilon}_i = \varepsilon_i + \lambda_i$, where λ_i is the Lagrange multiplier at quantum dot i. Because of the interaction between electrons, renormalized energies on dots depend on average occupations of electrons. On the other hand,

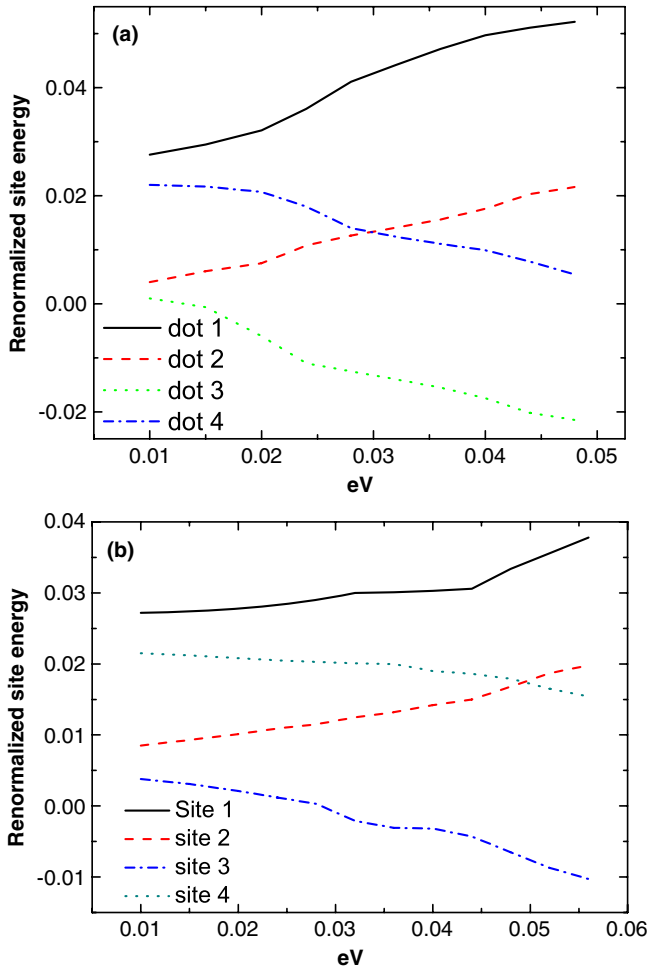

Figure 4. The renormalized energies of dots versus the bias between two leads when the dot number is four and (a) $t = 0.8$, (b) $t = 1.2$. The solid, dashed, dash–dotted, and dotted lines correspond to the energies at dots 1, 2, 3 and 4, respectively.

the coupling to the leads tends to draw the energies of dots, especially the dots near the leads, towards the Fermi levels of nearby leads. With the bias increasing, the renormalized energies at dots 1 and 2 increase while those at dots 3 and 4 drop nonlinearly due to the changing of the Fermi levels in the two leads. From the comparison of figures 4(a) and (b), we can see that by increasing the interdot hopping the difference in energy between the side dots (1 and 4) and the inner dots (2 and 3) decreases, reflecting the effect of the interdot hopping. On increasing the bias, the difference in energy between dots 2 and 3 increases, implying the weakening of the effective coupling between these two dots due to the bias.

Figures 5(a) and (b) show the curves of $\tilde{b}_i$ (the expectation value of b_i) versus the bias between two leads in the case of four dots for $t = 0.8$ and 1.2, respectively. One can see that when the bias increases, $\tilde{b}_1$ and $\tilde{b}_4$ increase and $\tilde{b}_2$ and $\tilde{b}_3$ drop, so $\tilde{t}_{1,2}$ (the renormalized intradot hopping between dot 1 and dot 2) and $\tilde{t}_{3,4}$ become much larger than $\tilde{t}_{2,3}$. Here, the expression $\tilde{t}_{i,i+1} = t\tilde{b}_N\tilde{b}_{N+1}$ is adopted. Thus, by increasing the bias, we can weaken the effective linking between two inner dots, but strengthen the links between the outer dots and the leads.

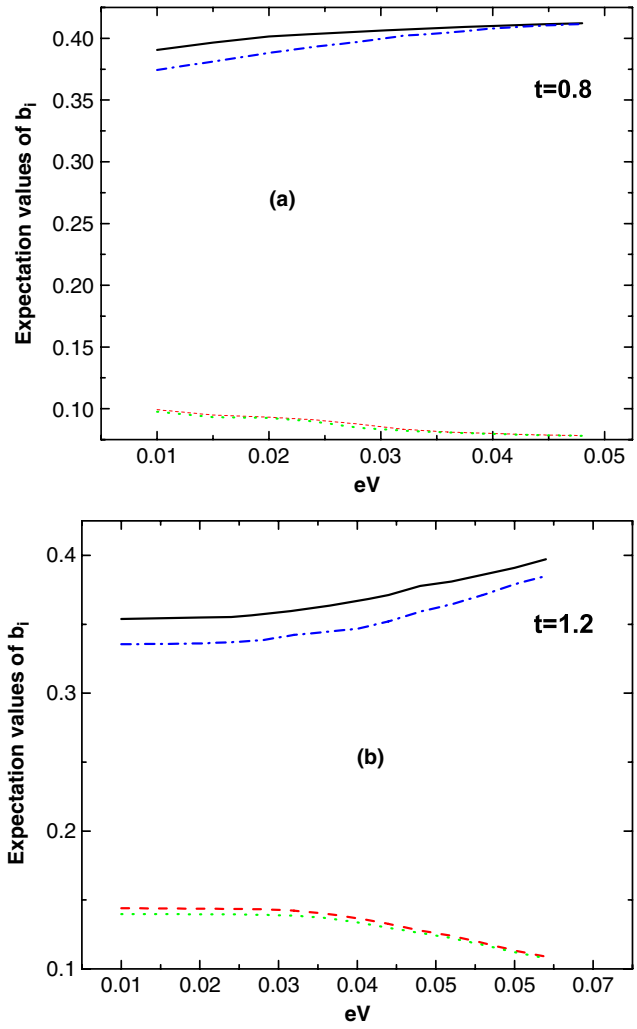

Figure 5. The expectation value of b_i versus the bias between two leads when the number of dots is four and (a) $t = 0.8$, (b) $t = 1.2$. The solid, dashed, dash–dotted, and dotted lines correspond to the expectation value of b_i at dot $i = 1, 2, 3$ and 4, respectively.

4. Conclusions

Using a slave-boson mean-field theory, we have shown that the combined effect of the dot–lead coupling and the interdot coupling in a series of quantum dots can widen and split the Kondo resonance peak in the curves of the differential conductance versus the bias voltage in comparison with the case of single quantum dot. When the number of dots is larger and the magnitude of the interdot coupling is of the order of the dot–lead coupling, some structures may appear in the Kondo resonance peak, and NDC occurs. It is also shown that the bias voltage at which the NDC appears depends strongly on the strength of the interdot coupling and on the number of quantum dots. It is also found that the conductance as a function of the interdot hopping shows two different scenarios in cases of odd and even dots, due to the different net spin of the isolated series. The obtained results may have a relation to experiments

which investigate the differential conductance through systems which can be regarded as series with more than one Kondo impurity. In the case of two dots, a split of the Kondo peak in the $\mathrm{d}I/\mathrm{d}V$–V curves was observed in recent measurements [20–22]. Sharp dips due to the negative differential conductance are still absent in the measurements; this may due to the dephasing processes [18].

Acknowledgments

This work was supported by National Foundation of Natural Science in China, Grant Nos 60676056 and 10474033, and by the China State Key Projects of Basic Research (2005CB623605).

References

[1] Goldhaber-Gordon D, Shtrikman H, Mahalu D, Abusch-Magder D, Meirav U and Kastner M A 1998 *Nature* **391** 156
[2] Cronenwett S M, Oosterkamp T H and Kouwenhoven L P 1998 *Science* **281** 540
[3] Glazman L I and Raikh M E 1988 *JETP Lett.* **47** 452
[4] Glazman L I and Raikh M E 1988 *JETP Lett.* **47** 452
Ng T K and Lee P A 1988 *Phys. Rev. Lett.* **61** 1768
[5] Beenakker C W J 1997 *Rev. Mod. Phys.* **69** 731
[6] Alhassid Y 2000 *Rev. Mod. Phys.* **72** 895
[7] Xiong S-J and Ye X 1999 *Phys. Rev. Lett.* **83** 1407
[8] Hofstetter W, König J and Schoeller H 2001 *Phys. Rev. Lett.* **87** 156803
[9] Kobayashi K, Aikawa H, Katsumoto S and Iye Y 2002 *Phys. Rev. Lett.* **88** 256806
[10] Choi M-S, Lee M, Kang K and Belzig W 2004 *Phys. Rev.* B **70** 020502(R)
[11] Aono T, Eto M and Kawamura K 1998 *J. Phys. Soc. Japan* **67** 1860
[12] Aono T and Eto M 2001 *Phys. Rev.* B **63** 125327
[13] Aono T and Eto M 2001 *Phys. Rev.* B **64** 073307
[14] Georges A and Meir Y 1999 *Phys. Rev. Lett.* **82** 3508
[15] Aguado R and Langreth D C 2000 *Phys. Rev. Lett.* **85** 1946
[16] Izumida W and Sakai O 2000 *Phys. Rev.* B **62** 10260
[17] Büsser C A, Anda E V, Lima A L, Davidovich M A and Chiappe G 2000 *Phys. Rev.* B **62** 9907
[18] Sánchez D and López R 2005 *Phys. Rev.* B **71** 035315
[19] Oguri A and Hewson A C 2005 *J. Phys. Soc. Japan* **74** 988
[20] Oosterkamp T H, Fujisama T, van der Wiel W G, Ishibashi K, Hijman R V, Tarucha S and Kouwenhoven L P 1998 *Nature* **395** 873
[21] Jeong H, Chang A M and Melloch M R 2001 *Science* **293** 2221
[22] van der Wiel W G, De Franceschi S, Elzerman J M, Fujisawa T, Tarucha S and Kouwenhoven L P 2003 *Rev. Mod. Phys.* **75** 1
[23] López R and Sánchez D 2003 *Phys. Rev. Lett.* **90** 116602
[24] Haug H and Jauho A-P 1996 *Quantum Kinetics in Transport and Optics of Semiconductors* (Berlin: Springer)
[25] Rudziński W, Barnaś J, Świrkowicz R and Wilczyński M 2005 *Phys. Rev.* B **71** 205307
[26] Dong B and Lei X L 2002 *Phys. Rev.* B **65** R241304
[27] de la Vega L, Martin-Rodero A, Yeyati A L and Saúl A 2004 *Phys. Rev.* B **70** 113107